



Contents lists available at ScienceDirect

## Deep-Sea Research Part I

journal homepage: [www.elsevier.com/locate/dsri](http://www.elsevier.com/locate/dsri)

## Factors that affect the nearshore aggregations of Antarctic krill in a biological hotspot



Kim S. Bernard<sup>a,\*</sup>, Megan Cimino<sup>b</sup>, William Fraser<sup>c</sup>, Josh Kohut<sup>d</sup>, Matthew J. Oliver<sup>e</sup>, Donna Patterson-Fraser<sup>c</sup>, Oscar M.E. Schofield<sup>d</sup>, Hank Statscewich<sup>f</sup>, Deborah K. Steinberg<sup>g</sup>, Peter Winsor<sup>f</sup>

<sup>a</sup> College of Earth, Ocean, and Atmospheric Sciences, Oregon State University, Corvallis, OR, USA

<sup>b</sup> Scripps Institution of Oceanography, USA

<sup>c</sup> Polar Oceans Research Group, USA

<sup>d</sup> Rutgers University, USA

<sup>e</sup> University of Delaware, USA

<sup>f</sup> University of Alaska, Fairbanks, USA

<sup>g</sup> Virginia Institute of Marine Science, College of William & Mary, USA

### ARTICLE INFO

#### Keywords:

Antarctic krill  
Euphausia superba  
Aggregation  
Biological hotspots  
Physical-biological interactions  
Wind  
Tide

### ABSTRACT

Antarctic krill, *Euphausia superba*, is a highly abundant and ecologically important zooplankton species in the Southern Ocean. Regions of elevated Antarctic krill biomass exist around Antarctica, often as a result of the concentrating effect of bathymetry and ocean currents. Such areas are considered biological hotspots and are key foraging grounds for numerous top predators in the region. A hotspot of Antarctic krill biomass exists off the southern extent of Anvers Island, Western Antarctic Peninsula, and supports a population of Adélie penguins that feed almost exclusively on it, as well as numerous other top predators. We investigated the spatio-temporal variability in Antarctic krill biomass and aggregation structure over four consecutive summer seasons, identifying environmental factors that were responsible. We identified three distinct krill aggregation types (Large-dense, Small-close and Small-sparse), and found that the relative proportion of each type to total aggregation numbers varied significantly between survey days. Large-dense aggregations occurred more frequently when westerly winds predominated and when the local mixed tide was in the diurnal regime. Small-close aggregations were also more frequent during diurnal tides and were negatively correlated with phytoplankton biomass. Small-sparse aggregations, on the other hand, were more prevalent when the mixed tide was in the semi-diurnal phase. We suggest that, under certain conditions (i.e. diurnal tides and westerly winds), the biological hotspot in the nearshore waters off Palmer Station, Anvers Island, functions as a zone of accumulation, concentrating krill biomass. Our findings provide important information on the dynamics of Antarctic krill at the local scale.

### 1. Introduction

In the ocean, biological hotspots are regions of elevated biomass that persist at decadal to centennial time scales (Schofield et al., 2013). These regions are known for their capacity to support high densities of avian, pinniped and cetacean predators that have evolved to recognize and make use of available resources (Palacios et al., 2006; Santora and Veit, 2013). In Antarctica, biological hotspots often exist where bathymetry and ocean currents interact to concentrate Antarctic krill (*Euphausia superba*, hereafter referred to as krill), the primary prey source to numerous top predators in the area (Chapman et al., 2010; Nicol et al., 2008; Nowacek et al., 2011; Santora et al., 2009, 2010;

Warren et al., 2009). Along the Western Antarctic Peninsula (WAP), one such hotspot exists off the southern extent of Anvers Island, extending from the nearshore waters out to Palmer Deep Canyon (Schofield et al., 2013). At Anvers Island, breeding Adélie penguins (*Pygoscelis adeliae*) feed almost exclusively on krill (Fraser and Hofmann, 2003). During the breeding season (austral spring-summer), adult Adélie penguins depend on the predictable resources of krill within their foraging range to provision their chicks (Fraser and Hofmann, 2003; Nicol et al., 2008; Wienecke et al., 2000).

Although south of Anvers Island persists as a biological hotspot over long ecological time scales, at shorter time scales (days to weeks) krill are highly patchy and ephemeral, and their biomass and availability (a

\* Corresponding author at: College of Earth, Ocean, and Atmospheric Sciences, Oregon State University, Corvallis, OR, USA.  
E-mail address: [kbernard@coas.oregonstate.edu](mailto:kbernard@coas.oregonstate.edu) (K.S. Bernard).

function of the type of aggregations formed) to predators can be strongly influenced by the local physical environment (Bernard and Steinberg, 2013; Brierley et al., 2006; Cox et al., 2011; Warren et al., 2009). Krill form aggregations of varying size and packing density that can be found throughout the water column either sparsely or densely spaced together (Bernard and Steinberg, 2013; Cox et al., 2011; Hamner and Hamner, 2000; Krafft et al., 2012; Tarling et al., 2009). Krill aggregation characteristics (e.g. shape, size, packing density, depth) are spatially heterogeneous even at the sub-mesoscale ( $< 1$  km), and, at a local scale, the types of aggregations present may change daily (Bernard and Steinberg, 2013). Variability in krill aggregations can impact foraging behavior in penguins and other top predators (Alonzo et al., 2003; Cimino et al., 2016; Grünbaum and Veit, 2003; Mori and Boyd, 2004). Shallow aggregations of krill minimize surface recovery time in diving penguins, allowing them to spend more time submerged foraging (Chappell et al., 1993; Kooyman, 1989). Encounter rates are greater when aggregations are larger and shallower, and thus more easily seen by visual predators (Grünbaum and Veit, 2003; Jansen et al., 1998). Various reasons have been proposed to explain aggregation behavior of krill, including reproduction, feeding, predator avoidance and energetic benefits (Hamner et al., 1983; Ritz, 2000), and it is possible that these reasons may become more or less important throughout the krill life cycle.

There are a number of possible physical mechanisms that might alter zooplankton biomass and availability to predators in biological hotspots on a daily basis, including tides and currents (Bernard and Steinberg, 2013; Lavoie et al., 2000; Murison and Gaskin, 1989), and strong wind events and storms (Batchelder et al., 1995; Jiang et al., 2007; Warren et al., 2009). The Adélie penguins breeding near Anvers Island exhibit daily variability in their foraging distances that has been correlated to tidal regime (Oliver et al., 2013). The tides at Anvers Island alternate between diurnal (one high and one low tide per day) and semi-diurnal (two high and two low tides per day) regimes on a roughly two-week basis (Amos, 1993), and Oliver et al. (2013) found that the foraging distance of Adélie penguins during semi-diurnal tides was roughly double that of diurnal tides. Bernard and Steinberg (2013) showed that krill biomass was also dependent on the local tidal regime with significantly higher biomass in the nearshore waters off Anvers Island during diurnal tides. This suggests that the penguins are responding to their prey. The latter study, however, did not resolve the underlying mechanisms by which diurnal tides resulted in increased krill biomass.

Here we describe variability in krill biomass and their availability to predators and suggest the physical mechanisms responsible. While krill within this region are important prey items for many top predators, we will concentrate the discussion of our results within the context of Adélie penguin foraging.

## 2. Methods

### 2.1. Study site

The study was conducted during the austral summers of 2011–2012, 2012–2013, 2013–2014, and 2014–2015 in the nearshore waters off Palmer Station, Anvers Island (Western Antarctic Peninsula, Fig. 1). Just southwest of Anvers Island, the across-shelf Palmer Deep Canyon comes to a head (Fig. 1, top right). The bathymetry then rises rapidly into the nearshore waters off Palmer Station, characterized by numerous small islands and shoals (Fig. 1, bottom right).

### 2.2. Acoustic sampling protocol

Krill were mapped acoustically from a  $\sim 6$  m Zodiac Mark V inflatable boat (*Ms. Chippy*) using a 120 kHz single frequency DT-X echo sounder from Biosonics. Acoustic surveys were conducted as frequently as possible during each summer season, however weather and sea ice

conditions restricted the total number of survey days (see Supplementary materials Tables 1–4 for details on survey dates). Surveys that were cut short due to changes in conditions (weather and/or sea ice) were excluded from our analysis since in those situations noise from waves and/or transiting through sea ice resulted in poor quality acoustic data. Survey grids differed between seasons, but were consistent within each season (Fig. 2) and we have taken this into consideration in our analyses (see further details in Section 2.7).

### 2.3. Krill length-frequencies

In order to get an estimate of population demographics in the region during our study, krill were collected each January from the ARSV *Laurence M. Gould* using a  $2 \times 2$  m square frame Metro net (700  $\mu$ m mesh size) towed obliquely through the water column to  $\sim 120$  m over Palmer Deep (see Fig. 1 for location marked by “X”), which is within 20 km of our study area (Steinberg et al., 2015). Length measurements were made for a subsample of at least 100 individuals randomly selected from each catch (see Supplementary materials Table 5 for catch information), using Standard Length 1 (SL1) for total length according to Mauchline (1970). Measured krill were binned into 1 mm length increments, ranging from 10 to 65 mm.

### 2.4. Acoustic data collection and processing

The acoustic data collection and processing approach is described in more detail in Bernard and Steinberg (2013). Briefly, the calibrated echo sounder was towed horizontally at a depth of  $\sim 1$  m at speeds of 3–5 knots. Volume backscattering strength ( $S_v$ ) measurements were binned vertically into 1 m bins, but to maintain spatial resolution on the horizontal plain, we did not bin pings at this stage. We used maximum ping rates of 5 pings per second. Krill were identified from other possible sources of scattering where volume backscattering strength at 120 kHz exceeded the  $-70$  dB threshold. An element in the acoustic matrix that qualified as krill, based on the threshold, was considered part of an aggregation if any of its eight neighboring elements also qualified as krill (Lawson et al., 2008b). Neighboring elements classified as krill were grouped into aggregations using the Image Processing Toolbox in MATLAB (R2014a). Aggregations smaller than  $2 \times 2$  m were discarded from further analysis to reduce the chance of incorrectly assigning backscatter signal from other scatterers (e.g. small fish) to krill. Identified krill aggregations were also visually examined and compared to the corresponding echograms to manually remove any that may have been caused by non-krill scatterers. Another possible scatterer with a similar volume backscattering strength to krill ( $-85$  to  $-65$  dB at 120 kHz) that might have influenced our acoustic signal is the tunicate, *Salpa thompsoni*, in its aggregate stage (Wiebe et al., 2010). Unlike krill, *S. thompsoni* does not form cohesive aggregations, but rather forms layers. When we passed over scattering layers identified during our surveys using the echo sounder, we conducted net tows from *Ms. Chippy* using a 1 m diameter ring net (2 mm mesh size) to validate potential krill aggregations (Bernard and Steinberg, 2013). These net tows were typically shallow (top 20 m) and relatively fast to minimize net avoidance. Note that, in contrast to ship-based acoustic surveys, working from a Zodiac has a number of constraints and it was not possible to tow the ring net through deeper aggregations encountered from *Ms. Chippy*. However, we were able to effectively sample the layers that could have been salps and in all instances, we only ever caught krill. When we passed over vast shallow layers, krill could often be seen visually from the side of the Zodiac.

#### 2.4.1. Target strength estimates

We used the Distorted-Wave Born Approximation (DWBA) model of Lawson et al. (2006) to predict target strengths (TS; units of dB re:  $1$  m<sup>2</sup>) for each 1 mm binned length category of krill. The model was parameterized with measured values of krill lengths and cylindrical

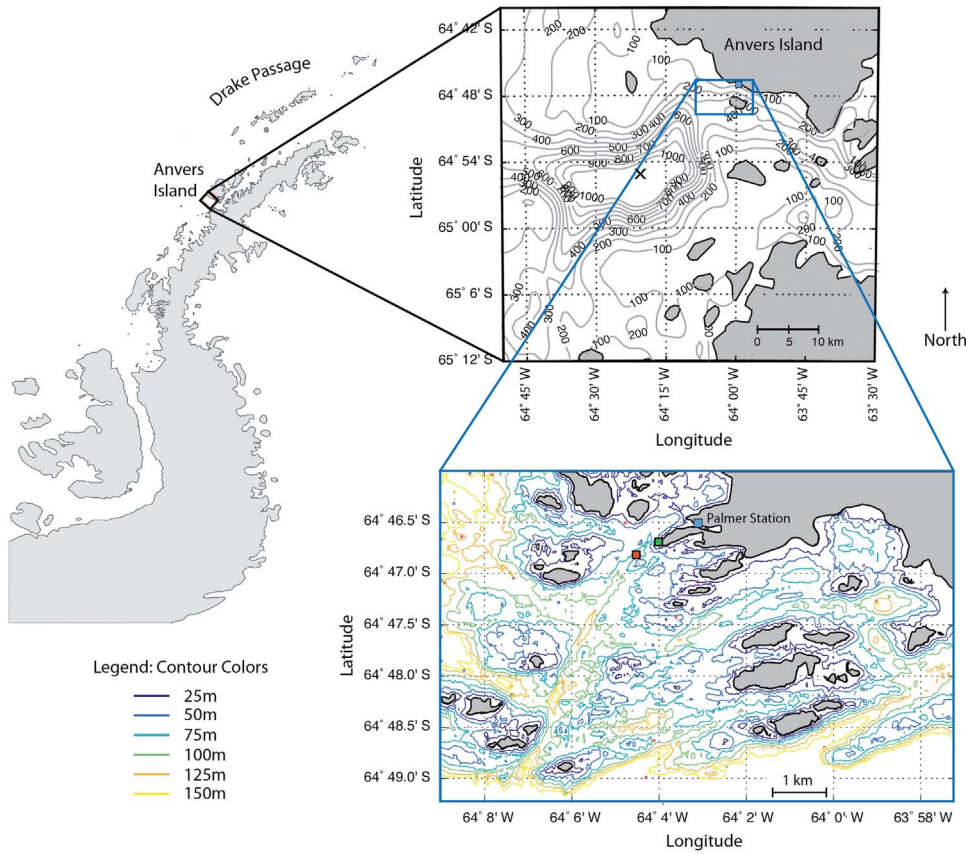


Fig. 1. Map of study area showing location of Anvers Island in relation to the Antarctic Peninsula (left panel), Palmer Deep Canyon (the center of which is denoted by the “X”, top right panel), and detailed bathymetry off Palmer Station (denoted by the blue square), Anvers Island (bottom right panel). The meteorological station is located on Gamage Point (denoted by the green square, bottom right panel) and the Chl-*a* samples were collected at PAL LTER Station B (denoted by the red square, bottom right panel). (For interpretation of the references to color in this figure legend, the reader is referred to the web version of this article.)

radii and with values of acoustic material properties ( $g$  and  $h$ ) calculated using regression equations obtained from the literature (Chu and Wiebe, 2005). Krill lengths were converted to SL2 from SL1 using the equations provided in Lawson et al. (2006). The ratio of length to cylindrical radius, 9.5, was calculated from net samples (Bernard and Steinberg, 2013). The model was set to estimate TS for a mean orientation of  $20^\circ$  (standard deviation of  $20^\circ$ ) after Lawson et al. (2004) and Chu et al. (1993). TS was then used to calculate backscattering cross-section  $\langle \sigma_{bs} \rangle$  where

$$TS = 10 \log_{10} \langle \sigma_{bs} \rangle \quad (1)$$

#### 2.4.2. Krill biomass estimates

Krill biomass estimates were made following Lawson et al. (2008b). Volume backscattering strength ( $S_v$ ) measurements were converted to volume backscattering coefficients ( $s_v$ ) following the equation,

$$S_v = 10 \log_{10} (s_v) \quad (2)$$

The values of  $s_v$  are the result of the sum of the product of  $\langle \sigma_{bs} \rangle_j$  of a single krill in size class  $j$  and the number ( $n_j$ ) of individuals per unit volume in that size class for all  $M$  size classes such that,

$$s_v = \sum_{j=1}^M \langle \sigma_{bs} \rangle_j n_j \quad (3)$$

The number of individuals in each size class ( $n_j$ ) is equal to the product of the total number of individuals ( $N$ ) across all  $M$  size classes and the fraction of individuals ( $P_j$ ) in size class  $j$ . Following this, Eq. (3) becomes

$$s_v = N \sum_{j=1}^M \langle \sigma_{bs} \rangle_j P_j \quad (4)$$

Krill abundance ( $N$ , ind.  $m^{-3}$ ) can then be solved since all other variables are known. Krill biomass ( $\rho$ ,  $g \ m^{-3}$ ) can be estimated as the

sum across all  $M$  size classes of the product of the wet-weight biomass of an individual krill in size class  $j$  ( $WW_j$ ,  $g$ ), the fraction of krill in each size class ( $P_j$ ), and the total abundance of krill ( $N$ , ind.  $m^{-3}$ ) (Lawson et al., 2008b), such that,

$$\rho = N \sum_{j=1}^M WW_j P_j \quad (5)$$

#### 2.5. Defining aggregation characteristics

During our four survey seasons, a total of 5858 krill aggregations (identified as described in *Acoustic data collection and processing*, above) were examined and key features, including mean depth (m), mean size (height  $\times$  length,  $m^2$ ), and mean biomass ( $g \ m^{-3}$ ) were described (Table 1). Nearest neighbor distances (NNDs, m) between aggregations were also described. For NNDs, distances between each aggregation and every other aggregation encountered on a particular day were calculated, and NND was determined as the shortest Euclidean distance between an aggregation and any other aggregation (Bernard and Steinberg, 2013). Note that the echo sounder had a maximum range of 250 m, below which any potential krill aggregations would not have been detected. Since short sections of our survey grids were over bottom depths  $> 250$  m, it is possible that our analysis missed deeper krill aggregations. However, this is likely insignificant since other studies have shown that aggregations of krill are typically within the top 100 m of the water column (Fielding et al., 2012; Warren and Demer, 2010).

#### 2.6. Environmental variables

Wind data were measured daily at the meteorological station situated on Gamage Point, Palmer Station (Fig. 1). Tidal regime was determined using a tide prediction algorithm developed specifically for

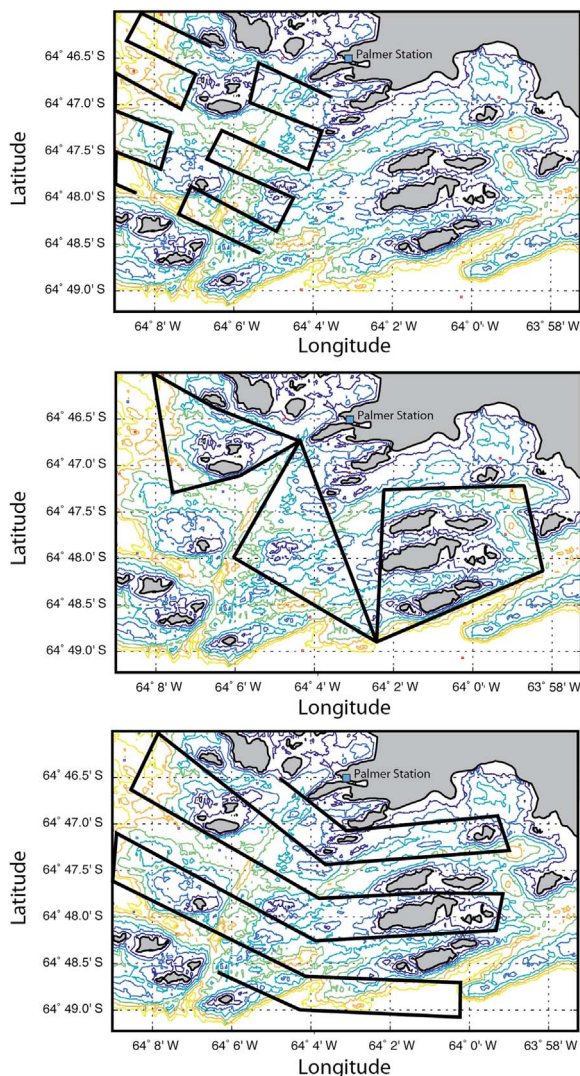


**Fig. 2.** Map showing acoustic survey grids occupied in 2011–2012 (top panel), 2012–2013 (middle panel), and 2013–2014 & 2014–2015 (bottom panel). Note that in 2013–2014 and 2014–2015, the same grid was occupied. The contour color legend is the same as in Fig. 1. (For interpretation of the references to color in this figure, the reader is referred to the web version of this article.)

**Table 1**

Features used to describe aggregation structure and the equations used to define them.  $D$  is depth;  $n$  is number of vertical bins;  $d_{jmax}$  is depth at maximum horizontal bin  $j$  for  $i$ th vertical bin;  $d_{jmin}$  is depth at minimum horizontal bin  $j$  for  $i$ th vertical bin;  $H$  is height;  $L$  is length;  $m$  is number of horizontal bins;  $l_j$  is length at  $j$ th horizontal bin;  $KE$  is krill extent;  $H_i$  is height at  $i$ th vertical bin;  $b_i$  is bottom depth at  $i$ th vertical bin;  $DSF$  is distance from sea floor;  $DSS$  is distance from sea surface;  $B$  is biomass;  $B_{ij}$  is biomass at coordinate of  $i$ th vertical bin and  $j$ th horizontal bin.

Aggregation Feature	Equation
Depth (m)	$D = \left[ \sum_{i=1}^n \left( \left( \frac{d_{ijmax} - d_{ijmin}}{2} \right) + d_{ijmin} \right) \right] \div n$
Height (m)	$H = \left[ \sum_{i=1}^n (d_{ijmax} - d_{ijmin}) \right] \div n$
Length (m)	$L = \left[ \sum_{j=1}^m (l_j) \right] \div m$
Biomass (g m <sup>-3</sup> )	$B = \left[ \sum_{i=1}^n \sum_{j=1}^m (B_{ij}) \right] \div n * m$

Palmer Station (Amos, 1993), as the tide gauge available was faulty during part of our study, and was based strictly on the number of high and low peaks per 24-h day (diurnal = 2 peaks, semi-diurnal = 1 peak). We also have included chlorophyll-*a* (chl-*a*) data obtained from the Palmer Antarctica Long-Term Ecological Research (PAL LTER) project in our analyses. Briefly for chl-*a*, seawater samples taken from 0, 5, 10, 20, 30 and 50 m depth at PAL LTER Station B (Fig. 1) were filtered onto Whatman GF/F filters, pigments were extracted in 90% acetone, and fluorescence measurements were made using a Turner Designs 10AU fluorometer (JGOFS, 1994). Since chl-*a* was not measured daily by the PAL LTER, we used the values obtained from the closest sampling day (< 3 days) for each acoustic sampling day. Although the environmental data were obtained from single points within our larger acoustic sampling area, these sites can be considered as representative of our study area (Tortell et al., 2014).

## 2.7. Data analysis

### 2.7.1. Identifying aggregation types

Aggregations were grouped using a Principle Components Analysis (PCA) and a Partitioning Around Medoids (PAM) cluster analysis, after Kaufman and Rousseeuw (1990). A PCA was carried out on centered and normalized aggregation parameters (i.e. depth, size, biomass and NND). The PAM cluster analysis was then performed on the results of the PCA. The silhouette validation method was used to select the number of clusters ( $k$ ) set *a priori* (Grebmeier et al., 2006). Eigenvectors of the first three principle components were used to identify aggregation parameters that were responsible for the clustering. Where the absolute value of an eigenvector element was greater than the product of 0.7 and the maximum absolute eigenvector value for a given principle component, the parameter was considered to have a significant influence (Cox et al., 2011).

### 2.7.2. Daily variability in aggregations

Because our sampling grids covered a reduced area in our first survey year compared with the next three years (Fig. 2), we first tested for significant variability in average percent contributions of each identified aggregation type between the west and east sectors of our study area (marked by the -64.06°W line of longitude) during each of the latter three years. Results of a Kruskal-Wallis one-way analysis of variance showed that percent contribution of each aggregation type to the total was not significantly different between the east and west in each of the latter three survey years. Subsequently, all further analyses on krill aggregation types were conducted with the full dataset.

Daily variability in percent contribution of each identified aggregation type was determined using the non-parametric one sample Wilcoxon test with the null hypothesis that percent contribution on a given day does not differ from the median of 10 randomly selected percent contribution values. The null hypothesis was rejected if the median  $p$  value from 10,000 permutations was < 0.05.

### 2.7.3. Identifying possible environmental drivers

We used linear mixed effects models (LMMs) and the information-theoretic approach to determine the environmental predictor variables (described above) responsible for day-to-day variation in percent contribution of each identified aggregation type. The information-theoretic approach uses a filter criterion to compare a set of models selected *a priori* (Burnham and Anderson, 2002), avoiding the many biases associated with traditional model selection methods, such as stepwise regression (Whittingham et al., 2006). We tested for collinearity - the significant correlation between predictor variables - using variance inflation factors with an upper limit of 3 (O'Brien, 2007; Zuur et al., 2010) and found no collinearity between environmental factors. Seven *a priori* models were selected for the information-theoretic approach, each associated with a specific hypothesis (Table 2).

**Table 2**  
Hypotheses and corresponding models used in the information-theoretic approach.

Model	Expression	Hypothesis
M1	$\log_{10}(\text{chl})$	Type I and II aggregations are relatively more abundant when phytoplankton biomass is high. Type III aggregations show the opposite trend.
M2	$u + v$	Winds that result in the net onshore movement of surface waters will correspond with increased relative abundances of Type I and II aggregations and decreased relative abundances of Type III aggregations.
M3	tide	Type I and II aggregations are relatively more abundant during diurnal tides (tide = 1), while Type III aggregations are relatively more abundant during semi-diurnal tides.
M4	$u + v + \text{tide}$	Diurnal tides and winds interact to result in net onshore movement of surface waters, which results in relatively more Type I and II aggregations and relatively fewer Type III aggregations.
M5	tide + $\log_{10}(\text{chl})$	Diurnal tides promote conditions favorable to phytoplankton growth, resulting in increased relative occurrence of Type I and II aggregations and the opposite trend for Type III aggregations.
M6	$u + v + \log_{10}(\text{chl})$	Wind-induced upwelling in the nearshore promotes phytoplankton growth and consequently elevated phytoplankton biomass, resulting in greater relative abundances of Type I and II aggregations and the opposite trend for Type III aggregations.
M7	tide + $\log_{10}(\text{chl}) + u + v$	A combination of diurnal tides and suitable winds promote conditions favorable for phytoplankton growth and consequently elevated phytoplankton biomass, resulting in greater relative abundances of Type I and II aggregations and the opposite trend for Type III aggregations.

LMMs were fit with the nlme package using restricted maximum likelihood estimation (Pinheiro et al., 2006) in R (R Development Core Team 2014) and included a random intercept term for survey year to account for differences in both our sampling strategies (different survey grids used) and the krill population (years of high versus low recruitment). Since our samples were collected at irregularly spaced time intervals, the corCAR1 correlation function (nlme package) was used to fit a continuous autoregressive error structure and is useful for irregular time series (Pollitt et al., 2012). Since our sample size was small ( $n = 63$ ), the models were compared using Akaike Information Criteria (AIC) corrected for small sample sizes (AICc). The AICc allowed us to determine the most parsimonious model with the fewest terms that accounted for the most variation. Models with lowest AICc values and highest AICc weights were subject to further model validation, including tests for patterns between residuals and covariates. Once a model was validated (i.e. no patterns were observed between residuals and covariates), we considered the predictor variable with the largest absolute value of the t-statistic to contribute most to the model's fit of observed data (Kuhn and Johnson, 2013).

### 3. Results

#### 3.1. Krill recruitment index

In 2011–2012, the 10–20 mm size class dominated the krill population, which is indicative of a strong recruitment ( $RI = 0.80$ ; Fig. 3A). In the subsequent summers, the krill population was dominated by sequentially larger individuals (2012–2013: 25–35 mm; 2013–2014: 30–40 mm; 2014–2015: 40–50 mm), indicating the growth of the main cohort that was recruited in 2011–2012, as well as lack of new recruitment ( $RI = 0.13$ ,  $RI = 0.13$  and  $RI = 0.19$ , in 2012–2013, 2013–2014, and 2014–2015, respectively; Fig. 3B, C and D).

#### 3.2. Krill aggregation types

The PCA identified aggregation size and biomass as being largely responsible for variance along the first principle component axis (PC1), while biomass and NND were most important for PC2, and size and NND were important for PC3. The highest Silhouette Coefficient, 0.85, was obtained for  $k = 3$  clusters. Thus, the PAM analysis identified three distinctly different aggregation types (Table 3). Type I aggregations were significantly larger, and shallower, with higher krill biomass than either Type II or III ( $p < 0.05$  for all, Table 3). Type II aggregations were significantly deeper in the water column than either Types I or III; Type II aggregations had the lowest krill biomass and highest NND values ( $p < 0.05$  for all, Table 3). Type III aggregations were statistically smallest among the three types and had the greatest NND values

( $p < 0.05$  for all, Table 3). The predominant aggregation type varied significantly between survey days (one sample Wilcoxon test;  $p < 0.05$  for each aggregation type).

#### 3.3. Identifying possible environmental drivers

##### 3.3.1. Environmental variables

Wind direction and speed, as indicated by the  $u$  and  $v$  wind vectors, was highly variable throughout each season and was dominated by winds out of the south and west (one sample Wilcoxon test;  $p < 0.05$ , Supplementary materials, Figs. 1 and 2). Although peaks in Chl- $a$  were observed each survey season, values did not vary significantly between sampling days during any of the four surveys (one sample Wilcoxon test;  $p > 0.05$ , Supplementary materials, Fig. 3). During our study, tidal regime typically switched between diurnal and semi-diurnal roughly every two weeks.

##### 3.3.2. Model results – Type I aggregations

Of the seven *a priori* models, two suitable candidate models (M2 and M4) were identified (Table 4), and both models passed validation tests. M2 included  $u$  and  $v$  wind vectors, while M4 included both wind vectors and tidal regime (i.e. diurnal or semi-diurnal). When winds were strongly out of the south (i.e. positive  $v$  wind vectors), Type I aggregations were sparse (M2 t-statistic =  $-2.30$ ; M4 t-statistic =  $-2.48$ ). Type I aggregations were more frequently encountered when winds were predominantly westerly (i.e. positive  $u$  wind vectors) in direction (M2 t-statistic = 1.55; M4 t-statistic = 1.64). Diurnal tides also resulted in increased occurrence of Type I aggregations (M4 t-statistic =  $-1.22$ ).

##### 3.3.3. Model results – Type II aggregations

Three suitable candidate models (M5, M3 and M1) were identified for Type II aggregations (Table 4). However, only M5 and M3 passed validation tests, we thus discarded M1. M5 included tide and log-transformed Chl- $a$ ; M3 included only tide. Type II aggregations were more frequently encountered during diurnal tides (M5 t-statistic =  $-1.86$ ; M3 t-statistic =  $-1.65$ ). Our results also show that the number of Type II aggregations was negatively correlated with log-transformed Chl- $a$  (M5 t-statistic =  $-1.65$ ).

##### 3.3.4. Model results – Type III aggregations

The information theoretic approach produced two suitable models for Type III aggregations (M5 and M1, Table 4). These models both passed validation tests. M5 is described above for Type II aggregations, and M1 included log-transformed Chl- $a$  only. The opposite trends were observed with tide regime and log-transformed Chl- $a$  for Type III aggregations as were found for Type II aggregations. Type III aggregations

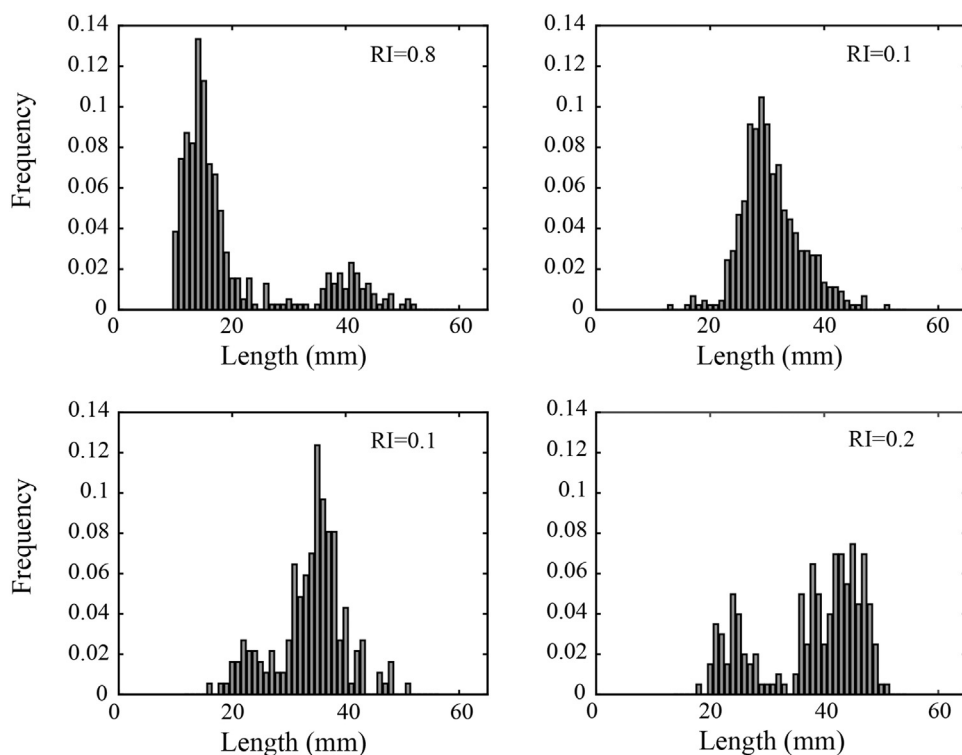


Fig. 3. Krill length frequencies in 1 mm length bins, for (A) 2011–2012, (B) 2012–2013, (C) 2013–2014, and (D) 2014–2015. Recruitment index (RI) is shown for each season.

were more frequently observed during semi-diurnal tides (M5 t-statistic = 1.88) and were positively correlated with log-transformed Chl-*a* (M5 t-statistic = 2.49; M1 t-statistic = 2.21).

#### 4. Discussion

Most studies examining spatial and temporal variability in Antarctic krill biomass and aggregation structure have been at the macro scale, spanning 10's to 100's of kilometers and seasons to years (see for example, Brierley et al., 1997; Fielding et al., 2014; Kinzey et al., 2015; Lawson et al., 2008a; Reiss et al., 2008; Ross et al., 2014; Steinberg et al., 2015). Though these studies provide valuable insights into the population dynamics of Antarctic krill, they do not yield sufficient resolution at the sub-mesoscale, the scale at which predators are affected over days to weeks. Our analysis of sub-mesoscale variability in krill aggregation structure, and thus their availability as prey to top predators, suggests significant fluctuations over relatively short time periods of days to weeks. We identified several key environmental variables that are, at least in part, responsible for these fluctuations.

Table 3

Mean (standard error) aggregation parameters for aggregation Types I–III identified with Principle Component Analysis and Partitioning Around Medoids analysis. Eigenvectors for the first three principle components (PC1–PC3) are provided for each aggregation parameter. The percent variation explained by each principle component is given in parentheses. Aggregation parameters with significant influence are highlighted in bold. NND is nearest neighbor distance. (For interpretation of the references to color in this table legend, the reader is referred to the web version of this article.)

Aggregation Parameter	Type I ( <i>n</i> = 2369)	Type II ( <i>n</i> = 1248)	Type III ( <i>n</i> = 2241)	PC1 (56.9 %)	PC2 (20.8 %)	PC3 (17.6 %)
Depth (m)	37 (0.5)	48 (0.5)	40 (0.7)	-0.020	0.074	0.187
Size (m <sup>2</sup> )	1419 (167)	104 (6)	67 (8)	<b>0.724</b>	0.143	<b>0.664</b>
Biomass (g m <sup>-3</sup> )	70 (2)	5 (0.1)	7 (0.2)	<b>0.604</b>	<b>-0.602</b>	-0.500
NND (m)	142 (5)	<b>22 (0.4)</b>	293 (10)	0.334	<b>0.782</b>	<b>-0.524</b>

We described three distinctly different aggregation types, each with their own unique set of characteristics. Type I aggregations were shallow (~37 m) and large (~1419 m<sup>2</sup>) with the highest krill biomass (~70 g m<sup>-3</sup>); throughout the remainder of our paper, we will refer to these as Large-dense aggregations. Type II aggregations were closely spaced together (~22 m), but were deeper (~48 m), on average, than Types I and III. Type II aggregations had low krill biomass (~5 g m<sup>-3</sup>), but due to their relatively larger size (~104 m<sup>2</sup>) would have had more krill overall than Type III aggregations that are significantly smaller (~67 m<sup>2</sup>) and that have relatively low biomass (~7 g m<sup>-3</sup>); we will refer to Type II aggregations as Small-close aggregations. Type III aggregations were small and had low krill biomass (averages given above); they were also relatively deep (~40 m) and were sparsely distributed (NND ~293 m). We will refer to Type III aggregations as Small-sparse aggregations.

Of the three aggregation types identified, Large-dense aggregations were most readily available to foraging Adélie penguins, while Small-sparse aggregations were the least readily available. Adélie penguins are central place foragers, and as such must balance energy expenditure (i.e. foraging time and effort) and energy intake (i.e. food consumption). During the breeding season, this is not only to ensure an animal meets its own metabolic requirements, but also that its young are sufficiently provisioned (Orlans and Pearson, 1979; Ydenberg et al., 1994). Krill aggregations that are large with high biomass (like our Large-dense aggregations) allow for maximum energy intake by foraging Adélie penguins. Adélie penguins are visual hunters and large aggregations are also more visible, enabling shorter search times between foraging bouts (Grünbaum and Veit, 2003; Jansen et al., 1998). Similarly, aggregations that are closely spaced together (i.e. low NND values) reduce search time for Adélies. Adélie penguins typically exhibit shallow hunting dives, often targeting the upper 40 m of the water column (Chappell et al., 1993; Cimino et al., 2016), thus shallower aggregations mean less energy expenditure in diving and a shorter surface recovery time (Chappell et al., 1993; Kooyman, 1989).

We found significant variability in the predominant aggregation type between survey days that could be described, at least in part, by key environmental predictor variables discussed in further detail below.

**Table 4**

Results from the linear mixed effects models used in the information-theoretic approach, showing Akaike's Information Criteria for small sample size (AICc), change in AICc ( $\Delta$ AICc), and AICc weights (AICw) for each aggregation type (Types I–III). The best model fits are highlighted in orange. (For interpretation of the references to color in this table legend, the reader is referred to the web version of this article.)

Model	Expression	Type I			Type II			Type III		
		AICc	$\Delta$ AICc	AICw	AICc	$\Delta$ AICc	AICw	AICc	$\Delta$ AICc	AICw
M1	chl	529.9	2.3	0.1	518.9	1.2	0.2	536.4	1.1	0.3
M2	u + v	527.6	0.0	0.3	523.0	5.2	0.03	542.5	7.2	0.01
M3	tide	529.9	2.3	0.1	518.2	0.5	0.3	539.0	3.7	0.1
M4	u + v + tide	528.5	0.9	0.2	523.0	5.2	0.03	541.8	6.5	0.02
M5	tide + chl	531.5	3.9	0.1	517.8	0.0	0.4	535.3	0.0	0.5
M6	u + v + chl	529.7	2.1	0.1	523.3	5.5	0.02	540.5	5.2	0.04
M7	tide + chl + u + v	530.5	2.9	0.1	522.6	4.9	0.03	538.5	3.2	0.1

#### 4.1. Effects of the environment on the occurrence of Large-dense aggregations

We found that the occurrence of Large-dense aggregations was dependent on wind speed and direction. During the summer months at Palmer Station, winds are primarily from the south, west or a combination of the two. Large-dense aggregations were more frequent when winds were predominantly out of the west. The proportion of Large-dense aggregations was, however, negatively correlated with southerly winds. Due to the orientation of Anvers Island, persistent westerly winds drive an onshore flow of surface waters as a result of Ekman transport. Coincident surface current measurements from a 3-site high frequency radar (HFR) system in January and February 2015 (Kohut et al., 2014) show the mean onshore flow during these westerly winds, from the head of the Palmer Deep Canyon towards Palmer Station (Fig. 4C). Submarine canyons are known to be regions of elevated biomass for euphausiids and small fishes (Allen et al., 2001; Genin, 2004; Lavoie et al., 2000; Mackas et al., 1997; Santora and Reiss, 2011) and we suggest that this onshore flow transports krill aggregations from the Palmer Deep Canyon into the nearshore region sampled by the acoustic surveys. Due to the bathymetry of the nearshore region (see Fig. 1), it is possible that krill brought inshore in this manner would accumulate, thereby elevating local krill biomass levels (Franks, 1992; Genin, 2004). Mean surface currents during southerly winds were weakly onshore toward Palmer Station (Fig. 4D). It is less clear how this would have resulted in proportionally fewer Large-dense aggregations. However, southerly winds were less common than westerly winds during the period when the HFR system was operating and they coincided more frequently with diurnal tides. At our study site, the tidal regime alternates between diurnal (single daily peak) and semi-diurnal (dual daily peaks) on a roughly a two-week basis. The HFR data clearly shows that the mean current direction across all diurnal tide days was onshore (Fig. 4A), while the mean over all semi-diurnal days was away from shore (Fig. 4B). It is possible then that the onshore mean surface current direction observed during southerly winds was determined more by tidal regime than wind in that period (January–February 2015).

Large-dense aggregations were observed more frequently during diurnal tides than they were during semi-diurnal tides. These findings suggest that during diurnal tides surface currents likely transport krill from the head of the Palmer Deep Canyon toward the nearshore waters off Palmer Station. During semi-diurnal tides, surface currents are directed away from our study site, removing krill from the nearshore waters. These findings are consistent with the higher krill biomass observed in the nearshore region during diurnal tides (Bernard and Steinberg, 2013).

#### 4.2. Effects of the environment on the occurrence of Small-close aggregations

Like Large-dense aggregations, Small-close aggregations were encountered most frequently during diurnal tides as opposed to semi-diurnal tides. Although these aggregations were not necessarily large and were relatively deep, they were numerous and closely spaced, and were within the average dive depth of Adélie penguins (i.e. ~40 m, Chappell et al., 1993; Cimino et al., 2016). Interestingly, the frequency of occurrence of Small-close aggregations was negatively correlated with phytoplankton biomass, suggesting that either (i) krill were avoiding areas of high phytoplankton biomass, or (ii) they were grazing at rates high enough to control phytoplankton stocks. Since krill are important grazers of phytoplankton, particularly during the spring and summer months when primary productivity is elevated and phytoplankton biomass is consequently high (Bernard et al., 2012), we suggest that the latter option is more likely. Indeed, in the same region one year prior to the start of our study, Cimino et al. (2016) found that krill aggregations occurred in areas with lower integrated Chl-*a*. At greater temporal scales in the same nearshore region, interannual peaks in krill abundances occurred in response to strongly positive spring/summer Chl-*a* anomalies the year before (Saba et al., 2014). Similarly, at a larger spatial scale, phytoplankton primary productivity was the main environmental control driving interannual summer abundances of Antarctic krill (with a 2-year lag) along the WAP study region of the PAL LTER (Steinberg et al., 2015). Chl-*a* is thus an important predictor of krill biomass at multiple scales.

#### 4.3. Effects of the environment on the occurrence of Small-sparse aggregations

Small-sparse aggregations responded with opposite trends to Large-dense and Small-close aggregations. Small-sparse aggregations were rarely encountered during diurnal tides, but rather dominated the aggregation types during semi-diurnal tides. We postulate that the predominant offshore current direction during semi-diurnal tides would have removed the majority of krill aggregations, leaving only few, sparsely distributed aggregations to remain. It is likely that in such a scenario, the low krill biomass in the nearshore waters would have released grazing pressure on phytoplankton standing stocks, thereby allowing Chl-*a* concentrations to rise. Indeed, our models showed a positive correlation between Small-sparse aggregations and Chl-*a*. Small-sparse aggregations were also negatively correlated with SST. While the mechanisms behind this are less clear, it is possible that low SST values may be indicative of increased through flow and mixing, conditions that may have dispersed krill aggregations, resulting in the predominance of only those that are small and sparse.

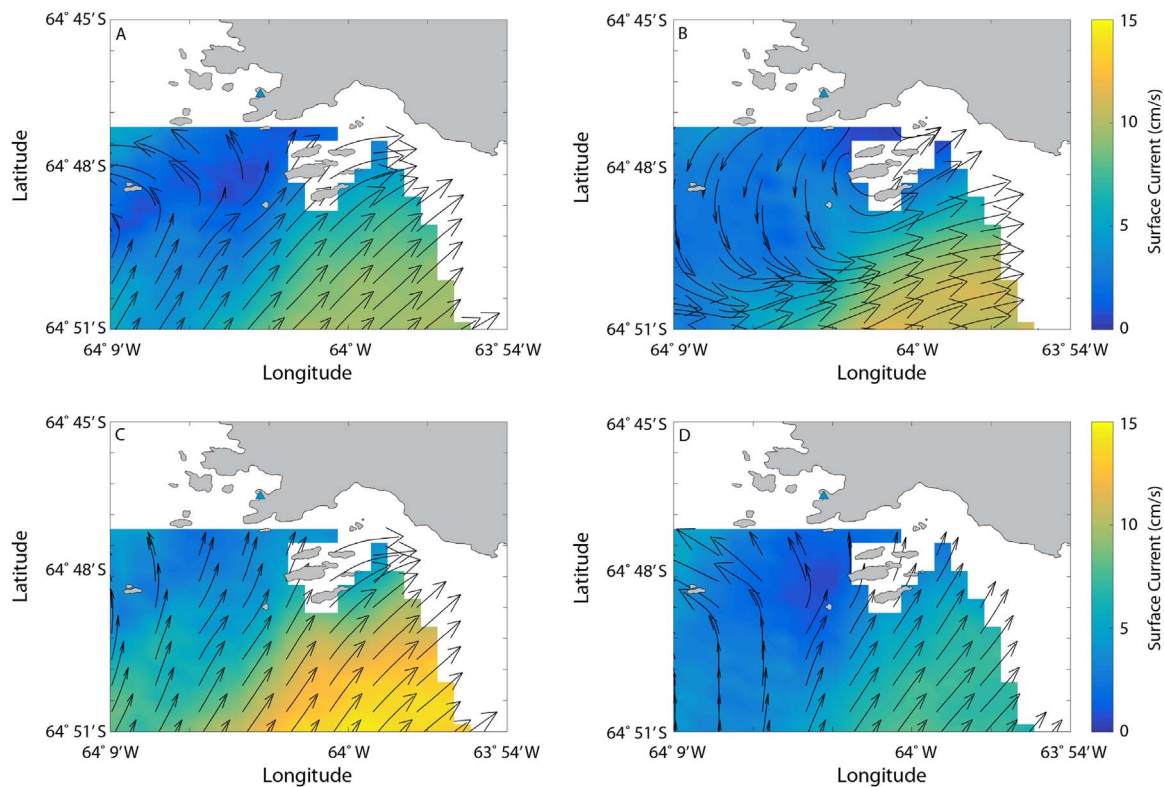


Fig. 4. Mean surface currents ( $\text{cm s}^{-1}$ ) in January and February 2015 during (A) diurnal tides, (B) semi-diurnal tides, (C) westerly winds, and (D) southerly winds. The blue triangle represents Palmer Station. (For interpretation of the references to color in this figure legend, the reader is referred to the web version of this article.)

## 5. Conclusion

We found that krill biomass and aggregation size were greatest during diurnal tides and when westerly winds predominated. Both conditions result in the net onshore flow of surface currents transporting waters from the Palmer Deep Canyon into the nearshore off Palmer Station, where the flow presumably interacts with bathymetry, resulting in accumulation of krill. Franks (1992) described the mechanisms by which biomass might accumulate at fronts, distinguishing between *retention* (characterized by closed particle streamlines) and *accumulation* (characterized by convergent particle streamlines) and noted that accumulation of strong swimmers, like krill, is likely. Given our findings presented above, we suggest that the nearshore waters off Palmer Station function as a zone of *accumulation* for krill during persistent westerly winds and diurnal tides.

## Acknowledgements

We are grateful to the Antarctic Services Company and the United States Antarctic Program for outstanding logistics, field and facilities support at Palmer Station. Dominique Paxton and Shenandoah Raycroft were exceptional field assistants and we could not have done the work without them. We appreciate the advice and assistance from A. Zuur on the information-theoretic approach. This study was funded by the US National Science Foundation (OPP-0823101, PLR-1440435, and PLR-1331681). This contribution is number 3636 from the Virginia Institute of Marine Science.

## Appendix A. Supporting information

Supplementary data associated with this article can be found in the online version at <http://dx.doi.org/10.1016/j.dsr.2017.05.008>.

## References

- Allen, S.E., Vindeirinho, C., Thomson, R.E., Foreman, M.G., Mackas, D.L., 2001. Physical and biological processes over a submarine canyon during an upwelling event. *Can. J. Fish. Aquat. Sci.* 58 (4), 671–684.
- Alonzo, S.H., Switzer, P.V., Mangel, M., 2003. Ecological games in space and time: the distribution and abundance of Antarctic krill and penguins. *Ecology* 84 (6), 1598–1607.
- Amos, A.F., 1993. RACER: the tides at Palmer station. *Antarct. J.* 28 (5), 162–164.
- Batchelder, H.P., VanKeuren, J.R., Vaillancourt, R., Swift, E., 1995. Spatial and temporal distributions of acoustically estimated zooplankton biomass near the Marine Light-Mixed Layers station (59°30'N, 21°00'W) in the North Atlantic in May 1991. *J. Geophys. Res.* 100 (C4), 6549–6563.
- Bernard, K.S., Steinberg, D.K., 2013. Krill biomass and aggregation structure in relation to tidal cycle in a penguin foraging region off the Western Antarctic Peninsula. *ICES J. Mar. Sci.* 70 (4), 834–849.
- Bernard, K.S., Steinberg, D.K., Schofield, O.M.E., 2012. Summertime grazing impact of the dominant macrozooplankton off the Western Antarctic Peninsula. *Deep-Sea Res.* 62, 111–122.
- Brierley, A.S., Saunders, R.A., Bone, D.G., Murphy, E.J., Enderlein, P., Conti, S.G., Demer, D.A., 2006. Use of moored acoustic instruments to measure short-term variability in abundance of Antarctic krill. *Limnol. Oceanogr.: Methods* 4, 18–29.
- Brierley, A.S., Watkins, J.L., Murray, A.W.A., 1997. Interannual variability in krill abundance at South Georgia. *Mar. Ecol. Progress. Ser.* 150, 87–98.
- Burnham, K.P., Anderson, D.R., 2002. *Model Selection and Multi-model Inference: A Practical Information-Theoretic Approach*. Springer, New York, NY.
- Chapman, E.W., Hofmann, E.E., Patterson, D.L., Fraser, W.R., 2010. The effects of variability in Antarctic krill (*Euphausia superba*) spawning behavior and sex/maturity stage distribution on Adélie penguin (*Pygoscelis adeliae*) chick growth: a modeling study. *Deep-Sea Res.* 57, 543–558.
- Chappell, M.A., Shoemaker, V.H., Janes, D.N., Bucher, T.L., Maloney, S.K., 1993. Diving behavior during foraging in breeding Adélie penguins. *Ecology* 74 (4), 1204–1215.
- Chu, D., Foote, K.G., Stanton, T.K., 1993. Further analysis of target strength measurements of Antarctic krill at 38 and 120 kHz: comparison with deformed cylinder model and inference of orientation distribution. *J. Acoust. Soc. Am.* 93 (5), 2985–2988.
- Chu, D., Wiebe, P.H., 2005. Measurements of sound-speed and density contrasts of zooplankton in Antarctic waters. *ICES J. Mar. Sci.* 62, 818–831.
- Cimino, M.A., Moline, M.A., Fraser, W.R., Patterson-Fraser, D.L., Oliver, M.J., 2016. Climate-driven sympatry may not lead to foraging competition between congeneric top-predators. *Nat. Sci. Rep.*
- Cox, M.J., Watkins, J.L., Reid, K., Brierley, A.S., 2011. Spatial and temporal variability in the structure of aggregations of Antarctic krill (*Euphausia superba*) around South Georgia, 1997–1999. *ICES J. Mar. Sci.* 68 (3), 489–498.

- Fielding, S., Watkins, J.L., Collins, M.A., Enderlein, P., Venables, H.J., 2012. Acoustic determination of the distribution of fish and krill across the Scotai Sea in spring 2006, summer 2008 and autumn 2009. *Deep-Sea Res. II* 59–60, 173–188.
- Fielding, S., Watkins, J.L., Trathan, P.N., Enderlein, P., Waluda, C.M., Stowasser, G., Tarling, G.A., Murphy, E.J., 2014. Interannual variability in Antarctic krill (*Euphausia superba*) density at South Georgia, Southern Ocean: 1997–2013. *ICES J. Mar. Sci.*
- Franks, P.J.S., 1992. Sink or swim: accumulation of biomass at fronts. *Mar. Ecol. Progress. Ser.* 82, 1–12.
- Fraser, W.R., Hofmann, E.E., 2003. A predator's perspective on causal links between climate change, physical forcing and ecosystem response. *Mar. Ecol. Progress. Ser.* 265, 1–15.
- Genin, A., 2004. Bio-physical coupling in the formation of zooplankton and fish aggregations over abrupt topographies. *J. Mar. Syst.* 50, 3–20.
- Grebmeier, J.M., Overland, J.E., Moore, S.E., Farley, E.V., Carmack, E.C., Cooper, L.W., Frey, K.E., Helle, J.H., McClaughlin, F.A., McNutt, S.L., 2006. A major ecosystem shift in the Northern Bering Sea. *Science* 311, 1461–1464.
- Grünbaum, D., Veit, R.R., 2003. Black-browed albatross foraging on Antarctic krill: density-dependence through local enhancement? *Ecology* 84 (12), 3265–3275.
- Hamner, W.M., Hamner, P.P., 2000. Behavior of Antarctic krill (*Euphausia superba*): schooling, foraging, and antipredatory behavior. *Cand. J. Fish. Aquac. Sci.* 57, 192–202.
- Hamner, W.M., Hamner, P.P., Strand, S.W., Gilmer, R.W., 1983. Behavior of Antarctic Krill, *Euphausia superba*: Chemoreception, feeding, schooling, and moulting. *Science* 220 (4595), 433–435.
- Jansen, J.K., Boveng, P.L., Bengtson, J.L., 1998. Foraging modes of chinstrap penguins: contrasts between day and night. *Mar. Ecol. Progress. Ser.* 165, 161–172.
- JGOFS, 1994. JGOFS Protocols. *Sci. Comm. Ocean. Res. Int. Counc. Sci. Unions* 210.
- Jiang, S., Dickey, T.D., Steinberg, D.K., Madin, L.P., 2007. Temporal variability of zooplankton biomass from ADCP backscatter time series data at the Bermuda testbed Mooring site. *Deep-Sea Res. I* 54, 608–636.
- Kaufman, L., Rousseeuw, P.J., 1990. *Finding Groups in Data: An Introduction to Cluster Analysis*. Wiley, New York.
- Kinzey, D., Watters, G.M., Reiss, C.S., 2015. Selectivity and two biomass measures in an age-based assessment of Antarctic krill (*Euphausia superba*). *Fish. Res.* 168, 72–84.
- Kohut, J., Bernard, K., Fraser, W., Oliver, M., Statscewich, H., Winsor, P., Miles, T., 2014. Studying the impacts of local oceanographic processes on Adélie penguin foraging ecology. *Mar. Technol. Soc. J.* 48 (5), 25–34.
- Kooyman, G.L., 1989. *Diverse Divers*. Springer-Verlag, Berlin, Germany.
- Krafft, B.A., Skaret, G., Knutsen, T., Melle, W., Klevjer, T., Søiland, H., 2012. Antarctic krill swarm characteristics in the Southeast Atlantic sector of the Southern Ocean. *Mar. Ecol. Progress. Ser.* 465, 69–83.
- Kuhn, M., Johnson, K., 2013. *Applied Predictive Modeling*. Springer, New York, NY.
- Lavoie, D., Simard, Y., Saucier, F.J., 2000. Aggregation and dispersion of krill at channel heads and shelf edges: the dynamics in the Saguenay - St. Lawrence marine park. *Canadian J. Fish. Aquac. Sci.* 57, 1853–1869.
- Lawson, G.L., Wiebe, P.H., Ashjian, C.J., Chu, D., Stanton, T.K., 2006. Improved parameterization of Antarctic krill target strength models. *J. Acoust. Soc. Am.* 119 (1), 232–242.
- Lawson, G.L., Wiebe, P.H., Ashjian, C.J., Gallager, S.M., Davis, C.S., Warren, J.D., 2004. Acoustically-inferred zooplankton distribution in relation to hydrography west of the Antarctic Peninsula. *Deep-Sea Res. II* 51, 2041–2072.
- Lawson, G.L., Wiebe, P.H., Ashjian, C.J., Stanton, T.K., 2008a. Euphausiid distribution along the Western Antarctic Peninsula - Part B: Distribution of euphausiid aggregations and biomass, and associations with environmental features. *Deep-Sea Res. II* 55, 432–454.
- Lawson, G.L., Wiebe, P.H., Stanton, T.K., Ashjian, C.J., 2008b. Euphausiid distribution along the Western Antarctic Peninsula - Part A: development of robust multi-frequency acoustic techniques to identify euphausiid aggregations and quantify euphausiid size, abundance, and biomass. *Deep-Sea Res. II* 55, 412–431.
- Mackas, D.L., Kieser, R., Saunders, M., Yelland, D.R., Brown, R.M., Moore, D.F., 1997. Aggregation of euphausiids and Pacific hake (*Merluccius productus*) along the outer continental shelf off Vancouver island. *Can. J. Fish. Aquac. Sci.* 54, 2080–2096.
- Mauchline, J., 1970. Measurement of body length of *Euphausia superba* Dana. *BIOMASS Handbook No. 4. SCAR/SCOR/IABO/ACMRR*, p. 9.
- Mori, Y., Boyd, I.L., 2004. The behavioral basis for nonlinear functional responses and optimal foraging in Antarctic fur seals. *Ecology* 85 (2), 398–410.
- Murison, L.D., Gaskin, D.E., 1989. The distribution of right whales and zooplankton in the Bay of Fundy, Canada. *Can. J. Zool.* 67, 1411–1420.
- Nicol, S., Clarke, J., Romaine, S.J., Kawaguchi, S., Williams, G., Hosie, G.W., 2008. Krill (*Euphausia superba*) abundance and Adélie penguin (*Pygoscelis adeliae*) breeding performance in the waters off the Béchervaise Island colony, East Antarctica in 2 years with contrasting ecological conditions. *Deep-Sea Res. II* 55, 540–557.
- Nowacek, D.P., Friedlaender, A.S., Halpin, P.N., Hazen, E.L., Johnston, D.W., Read, A.J., Espinasse, B., Zhou, M., Zhu, Y., 2011. Super-aggregations of krill and humpback whales in Wilhelmina Bay, Antarctic Peninsula. *PLoS One* 6 (4), e19173.
- O'Brien, R.M., 2007. A caution regarding rules of thumb for variance inflation factors. *Qual. Quant.* 41, 673–690.
- Oliver, M.J., Irwin, A., Moline, M.A., Fraser, W., Patterson, D., Schofield, O., Kohut, J., 2013. Adélie penguin foraging location predicted by tidal regime switching. *PLoS One* 8, 1.
- Orians, G.H., Pearson, N.E., 1979. On the theory of central place foraging. In: Horn, D.H., Mitchell, R.D., Stairs, G.R. (Eds.), *Analyses of Ecological Systems*. Ohio State University Press, Columbus, OH, pp. 155–177.
- Palacios, D.M., Bograd, S.J., Foley, D.G., Schwing, F.B., 2006. Oceanographic characteristics of biological hot spots in the North Pacific: a remote sensing perspective. *Deep-Sea Res. II* 53, 250–269.
- Pinheiro, J., Bates, D., DebRoy, S., Sarkar, D., 2006. nlme: an R package for fitting and comparing Gaussian linear and nonlinear mixed-effects models.
- Pollitt, L.C., Reece, S.E., Mideo, N., Nussey, D.H., Colegrave, N., 2012. The Problem of Auto-Correlation in Parasitology. *PLoS Pathog.* 8 (4), e1002590.
- Reiss, C.S., Cossio, A.M., Loeb, V., Demer, D.A., 2008. Variations in the biomass of Antarctic krill (*Euphausia superba*) around the South Shetland Islands, 1996–2006. *ICES J. Mar. Sci.* 65, 497–508.
- Ritz, D.A., 2000. Is social aggregation in aquatic crustaceans a strategy to conserve energy? *Can. J. Fish. Aquac. Sci.* 57 (S3), 59–67.
- Ross, R.M., Quetin, L.B., Newberger, T., Shaw, C.T., Jones, J.L., Oakes, S.A., Moore, K.J., 2014. Trends, cycles, interannual variability for three pelagic species west of the Antarctic Peninsula 1993–2008. *Mar. Ecol. Progress. Ser.* 515, 11–32.
- Saba, G., Fraser, W., Saba, V., Iannuzzi, R., Coleman, K., Doney, S., Ducklow, H., Martinson, D., Miles, T., Patterson-Fraser, D., Stammerjohn, S., Steinberg, D., Schofield, O., 2014. Winter and spring controls on the summer food web of the coastal West Antarctic Peninsula. *Nature Communications*.
- Santora, J.A., Reiss, C.S., 2011. Geospatial variability of krill and top predators within an Antarctic submarine canyon system. *Mar. Biol.* 158, 2527–2540.
- Santora, J.A., Reiss, C.S., Cossio, A.M., Veit, R.R., 2009. Interannual spatial variability of krill (*Euphausia superba*) influences seabird foraging behavior near Elephant Island, Antarctica. *Fish. Oceanogr.* 18 (1), 20–35.
- Santora, J.A., Reiss, C.S., Loeb, V.J., Veit, R.R., 2010. Spatial association between hotspots of baleen whales and demographic patterns of Antarctic krill *Euphausia superba* suggests size-dependent predation. *Mar. Ecol. Progress. Ser.* 405, 255–269.
- Santora, J.A., Veit, R.R., 2013. Spatio-temporal persistence of top predator hotspots near the Antarctic Peninsula. *Mar. Ecol. Progress. Ser.* 487, 287–304.
- Schofield, O., Ducklow, H., Bernard, K., Doney, S., Patterson-Fraser, D., Gorman, K., Martinson, D., Meredith, M., Saba, G., Stammerjohn, S., Steinberg, D., Fraser, W., 2013. Penguin biogeography along the West Antarctic Peninsula: testing the canyon hypothesis with Palmer LTER observations. *Oceanography* 26 (3), 204–206.
- Steinberg, D.K., Ruck, K.E., Gleiber, M.R., Garzio, L.M., Cope, J.S., Bernard, K.S., Stammerjohn, S.E., Schofield, O.M.E., Quetin, L.B., Ross, R.M., 2015. Long-term (1993–2013) changes in macrozooplankton off the Western Antarctic Peninsula. *Deep Sea Res. Part I: Oceanogr. Res. Pap.*
- Tarling, G.A., Klevjer, T., Fielding, S., Watkins, J., Atkinson, A., Murphy, E., Korb, R., Whitehouse, M., Leaper, R., 2009. Variability and predictability of Antarctic krill swarm structure. *Deep-Sea Res. I*.
- Tortell, P.D., Asher, E.C., Ducklow, H.W., Goldman, J.A.L., Dacey, J.W.H., Grzymiski, J.J., Young, J.N., Kranz, S.A., Bernard, K.S., Morel, F.M.M., 2014. Metabolic balance of coastal Antarctic waters revealed by autonomous pCO<sub>2</sub> and ΔO<sub>2</sub>/Ar measurements. *Geophys. Res. Lett.* 41, 6803–6810.
- Warren, J.D., Demer, D.A., 2010. Abundance and distribution of Antarctic krill (*Euphausia superba*) nearshore of Cape Shirreff, Livingston island, Antarctica, during six austral summers between 2000 and 2007. *Can. J. Fish. Aquac. Sci.* 67, 1159–1170.
- Warren, J.D., Santora, J.A., Demer, D.A., 2009. Submesoscale distribution of Antarctic krill and its avian and pinniped predators before and after a near gale. *Mar. Biol.* 156, 479–491.
- Whittingham, M.J., Stephens, P.A., Bradbury, R.B., Freckleton, R.P., 2006. Why do we still use stepwise modeling in ecological behaviour? *J. Anim. Ecol.* 75, 1182–1189.
- Wiebe, P.H., Chu, D., Kaartvedt, S., Hundt, A., Melle, W., Ona, E., Batta-Lona, P., 2010. The acoustic properties of *Salpa thompsoni*. *ICES J. Mar. Sci.* 67, 583–593.
- Wienecke, B.C., Lawless, R., Rodary, D., Bost, C.-A., Thomson, R., Pauly, T., Robertson, G., Kerry, K.R., LeMaho, Y., 2000. Adélie penguin foraging behaviour and krill abundance along the Wilkes and Adélie land coasts, Antarctica. *Deep-Sea Res. II* 47, 2573–2587.
- Ydenberg, R.G., Welham, C.V.J., Schmid-Hempel, R., Schmid-Hempel, P., Beauchamp, G., 1994. Time and energy constraints and the relationships between currencies in foraging theory. *Behav. Ecol.* 5, 28–34.
- Zuur, A.F., Ieno, E.N., Elphick, C.S., 2010. A protocol for data exploration to avoid common statistical problems. *Methods Ecol. Evol.* 1, 3–14.